

Electron-lattice coupling and the broken symmetries of the molecular salt $(\text{TMTTF})_2\text{SbF}_6$

W. Yu,^{1,*} F. Zhang,¹ F. Zamborszky,¹ B. Alavi,¹ A. Baur,² C. A. Merlic,² and S. E. Brown¹

¹*Department of Physics and Astronomy, University of California, Los Angeles, CA 90095*

²*Department of Chemistry and Biochemistry, University of California, Los Angeles, CA 90095*

(Dated: June 24, 2018)

$(\text{TMTTF})_2\text{SbF}_6$ is known to undergo a charge ordering (CO) phase transition at $T_{CO} \approx 156\text{K}$ and another transition to an antiferromagnetic (AF) state at $T_N \approx 8\text{K}$. Applied pressure P causes a decrease in both T_{CO} and T_N . When $P > 0.5\text{GPa}$, the CO is largely suppressed, and there is no remaining signature of AF order. Instead, the ground state is a singlet. In addition to establishing an expanded, general phase diagram for the physics of TMTTF salts, we establish the role of electron-lattice coupling in determining how the system evolves with pressure.

The isostructural family of charge transfer salts $(\text{TMTTF})_2X$ and $(\text{TMTSF})_2X$ are formed with singly charged anions, such as ClO_4^- , PF_6^- , and Br^- , so the average hole count is 0.5/donor. In the case of the TMTTF salts, they are susceptible to a charge-ordering (CO) transition at temperatures of the order of 100K ^{2,3}, which is often attributed to the importance of both on-site and near-neighbor Coulomb repulsion⁴, and influenced by electron-lattice coupling^{3,5,6,7,8}. Compared to the analog TMTSF materials, the bandwidths are much smaller, and therefore models naturally producing charge order and including only electronic degrees of freedom could be expected to describe some aspects of the physics correctly. Nevertheless, it is unclear whether realistic parameters successfully describe the experiments in several ways. First, it has been argued that the near-neighbor repulsion may not be strong enough to stabilize the charge order^{6,7,9}. Furthermore, although the charge-order (CO) order parameter has not been determined directly, there is indirect evidence from transport¹⁰ and EPR¹¹ measurements that the order-parameter's wavevector changes when the symmetry of the counterion is changed. An explanation should involve coupling of the charge degrees of freedom on the molecular stacks to the lattice. Calculations on one dimensional models including intramolecular, intermolecular, and counterion coupling indicate that when these degrees of freedom are included, a variety of new broken symmetry states are possible^{6,7,8}. At least in the case of the insulating TMTTF materials, it is not surprising that the robustness of the CO influences what ground state is observed¹². To date, very little is known about the details of the observed phases and what controls their stability.

The sensitivity to chemical or mechanical pressure of this class of materials provides an opportunity to explore some general trends. The pressure/temperature phase diagram for $(\text{TMTTF})_2\text{SbF}_6$ ¹³, determined using ¹³C NMR spectroscopy on spin-labeled crystals, appears in Fig. 1. As the pressure is increased, the ordering temperature T_{CO} to the CO state decreases. T_{CO} is reduced by almost half, to 90K , with 0.5GPa applied pressure. Over the same pressure range, the charge order amplitude is significantly reduced, and becomes unidentifiable

at pressures beyond it. As a consequence, the actual transition line is not established beyond 0.5GPa . Also decreasing is the AF ordering temperature T_N . When $P > 0.4\text{GPa}$, no experimental signature for the AF state is observed. For technical reasons associated with the experiments that are likely complicated by quenched disorder, we have not identified a phase boundary for the ground state found at high pressures. Rather, the results of experiments conducted in the range of $T = 2 - 5\text{K}$ exhibit the signatures of a singlet ground state¹³. Below, we describe experiments that demonstrate the role of the counterion sublattice in determining the observed phase diagram.

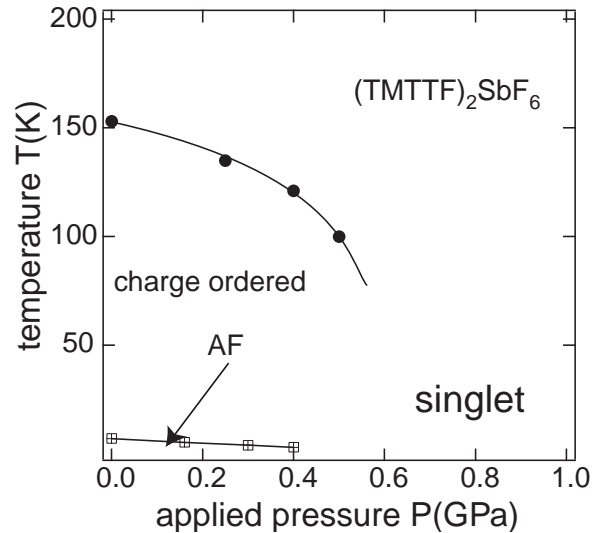


FIG. 1: Pressure vs. temperature phase diagram for $(\text{TMTTF})_2\text{SbF}_6$, identified using ¹³C NMR spectroscopy.

The samples were prepared as described previously. Spin-labeled TMTTF donors were synthesized with two ¹³C nuclei on the bridging sites at the center of the dimer molecules¹⁴, and subsequent crystal growth was carried out by electrolysis. The experiments consist of ¹³C and ¹⁹F NMR spectroscopy on $(\text{TMTTF})_2\text{SbF}_6$ as a function of pressure and temperature. In the first case, the external field was $B_0 = 9.0\text{T}$, with the field applied per-

pendicular to the \mathbf{a} (molecular stacking) axis. For the ^{19}F measurements, $B_0 = 4.9\text{T}$ was used. High pressure experiments were performed using a standard BeCu clamp cell using Flourinert 75 (3M) for the medium. The stated pressure, as shown in Fig. 1, is derived from the forces applied at $T = 300\text{K}$, and systematic consistency was verified using separate calibration runs.

Typical spectral changes are illustrated in Fig. 2, which shows the results of two-dimensional spin-echo spectroscopy¹⁵ ^{13}C NMR experiments. The experiment separates the hyperfine and chemical shifts from the internuclear dipolar coupling frequencies between pairs of neighboring ^{13}C nuclei¹⁶. The shifts are plotted on the vertical $f_2 - f_1$ axis, and the ^{13}C -dipolar coupling is shown on the horizontal f_1 axis. We note that the frequencies f_1 and f_2 result from the Fourier transform of the two dimensional data set in (t_1, t_2) , as defined in the figure. The spectrum taken with $T < T_{CO}$ is shown directly, and the spectrum for $T > T_{CO}$ is represented by the dark, open circles. Consider first the spectrum of the high-temperature phase. The signal appears at two frequencies on the $f_2 - f_1$ axis. When $T < T_{CO}$, the signal features multiply.

We understand the spectrum and how the changes pertain to charge disproportionation as follows². Within each molecule, there are two inequivalent ^{13}C sites, with distinct hyperfine couplings. This is the reason for signals appearing at two frequencies along the $f_2 - f_1$ axis in the high symmetry phase. Let's refer to them as ν_A (ν_B) for the higher (lower) frequency. The number of features are *doubled* in the CO phase because two inequivalent molecular environments develop, which we can label as α , β . As the NMR frequencies are related to the carrier densities on the α and β molecules, the frequency differences (*e.g.*, $\Delta\nu_A = \nu_{A\alpha} - \nu_{A\beta}$) are related to the CO order parameter. Some of the absorption features are unresolved in the spectrum shown. The inset shows the temperature dependence $\Delta\nu_B$, which saturates and then decreases upon cooling.

In Fig. 3 are shown ^{19}F spectra recorded over a range of temperatures. From approximately $T = 130\text{K}$ and below, changes in both the first moment and linewidth are noticeable. These are summarized in Fig. 4, where the linewidth is defined as the frequency span that includes half of the integrated intensity. Changes appear to occur in two steps, the first in a temperature range centered about $T = 120\text{K}$ and the second in a temperature range around $T = 75 - 80\text{K}$.

In discussing these results, we first consider the nature of the ^{19}F linewidth broadening. It is natural, at least in part, to consider the spectral effects as related to motion of the SbF_6^- counterion. More generally, the counterions of the TMTTF and TMTSF salts fall into two classes: centrosymmetric and non-centrosymmetric. In the first class are the hexafluorides PF_6^- , AsF_6^- , and SbF_6^- , and Br^- , and in the second are ClO_4 , FSO_3 , etc. All are small and compact; SbF_6^- is one of the largest, with the $F - \text{Sb} - F$ linear distance approximately 3.8\AA . At high

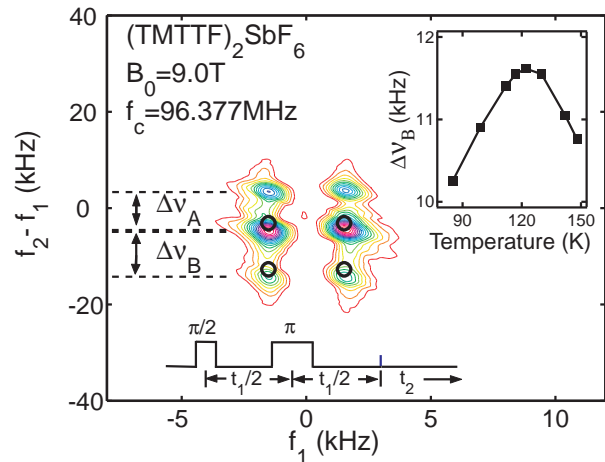


FIG. 2: ^{13}C NMR spectra at temperatures $T = 85\text{K} < T_{CO}$ (contours) and $T = 156\text{K} > T_{CO}$ (signal location represented by dark, open circles). The applied field is 9.0T directed in the $\mathbf{b}' - \mathbf{c}^*$ plane. In the inset is the temperature dependence of the frequency difference ($\Delta\nu$) of the peaks.

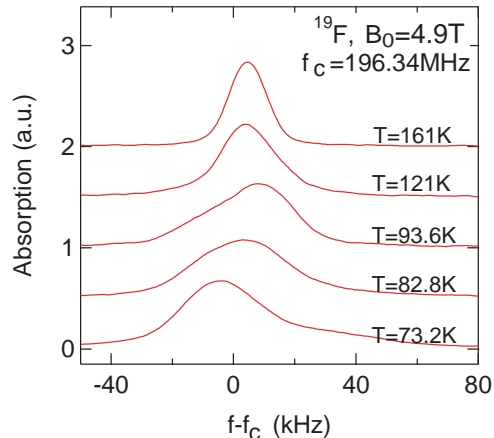


FIG. 3: Ambient pressure ^{19}F NMR spectra, recorded at different temperatures.

temperatures the orientation of the counterions is known to be highly disordered, and thought to be rotating¹⁷. Upon cooling, the non-centrosymmetric counterions orientationally order¹⁸ in a first order phase transition, lowering the space group symmetry of the crystal. The centrosymmetric ions are not reported to do that; instead, their motions are considered activated so linebroadening is expected to occur as a crossover upon cooling and there is no broken symmetry. At first glance, our results appear inconsistent with this scenario because the lineshape is asymmetric. In a single crystal, this would indicate highly disordered sites at low temperatures, and the resulting variation of chemical or Knight shifts. From the data, we see that a distribution of chemical shifts is not observable (the line is homogeneously broadened). Nevertheless, we do not rule out crystal twins as a con-

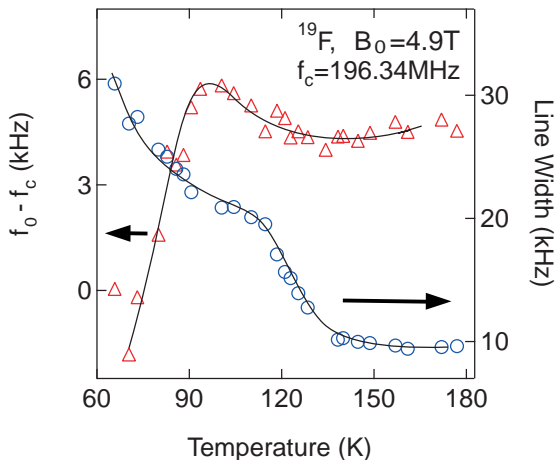


FIG. 4: First moment (^{19}F) and linewidth, evaluated from ^{19}F spectra as shown in Fig. 3. The first moment is measured relative to f_0 ; see the text for a definition of the linewidth. The solid lines serve as guides to the eye.

tributing factor in producing the observed lineshape. In either case, the broadening results when anionic motions become suitably slow or a first-order orientational ordering transition of some kind takes place. The second step in the ^{19}F linewidth appears to be associated with dynamics of some of the methyl groups and $^1\text{H} - ^{19}\text{F}$ coupling. As evidence, we note that there is a strong peak in the ^1H spin lattice relaxation in the same temperature range, and very similar in strength and temperature range to what is observed in the TMTSF salts¹⁷.

In this context, there is a natural association of the decrease in CO order parameter, from Fig. 2, with the ^{19}F line broadening and shift. For the broadening to occur, the anions must be stationary on a time scale of the order of the inverse (high-temperature) homogeneous linewidth¹⁹, which can occur through an activated diffusion process or as a result of a structural phase transition. For either case, the behavior of the order parameter suggests that suppression of counterion motion, or disorder associated with it, leads to suppression of the charge disproportionation on the donor molecules.

Finally, we address the evolution with pressure of both the CO order parameter and the ground states. In Fig. 1, neither the line demarking a transition to the CO phase, nor the CO/AF line is followed to $T = 0$. In transport experiments²⁰, there is an indication that the dielectric and resistive anomalies associated with the transition to the CO phase are monotonically suppressed with applied pressure. Our own transport studies confirm this. In the ^{13}C NMR spectrum, we observe some broadening of the spectral features, along with a weakening of the CO order parameter as pressure is increased. Beyond $P \approx 0.5\text{GPa}$, the CO features are unresolved. At the same time, the temperature at which ^{121}Sb linebroadening is observed coincides with the ^{19}F broadening and increases with pressure²¹. These observations suggest that there

is a phase competing with the CO, and its stability is associated with counterion degrees of freedom.

A natural first step is the quasi-one dimensional extended Hubbard model, including only electronic degrees of freedom⁴. With large enough on-site and near-neighbor repulsions U and V (relative to hopping integral t) in 1/4-filled systems, a charge pattern of alternating rich and poor sites is produced and the ground state is antiferromagnetic. Nevertheless, there are no diffraction experiments identifying the order parameter, and including electron-lattice coupling leads to other possibilities for the charge configuration of the CO state⁹. It is also argued that the physically appropriate values for V may not exceed the threshold for charge order. Nevertheless, producing ferroelectricity, as inferred from low-frequency dielectric experiments³, from the CO phase requires more couplings. Including the counterion naturally gives rise to ferroelectric order parameters^{6,8}. And Peierls-type coupling to the lattice leads to order parameters reminiscent of Spin-Peierls order^{5,22}. Then, it follows that a large-amplitude CO follows from coupling to the counterion and competes with the Peierls coupling and the SP ground state²³. Experimental evidence for the competition was seen previously in experiments on $(\text{TMTTF})_2\text{AsF}_6$ ¹². In the experiments reported here, the relative importance of the anion coupling is diminished once the anions freeze into place. That is, the freezing limits in some way the motion of the counterion. In turn, the coupling is reduced and the CO phase is destabilized.

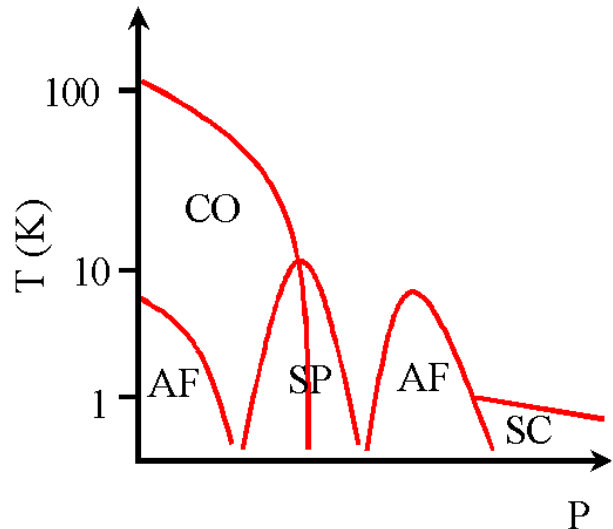


FIG. 5: A proposed generic phase diagram for the TMTTF and TMTSF salts.

To conclude, we offer a generic phase diagram for the TMTTF and TMTSF salts that incorporates our observations for the SbF_6 salt. At low chemical pressure, the donor stacks are strongly dimerized, T_{CO} is of the order 200K, and the ground state is antiferromagnetic. Increasing pressure leads to a frustration of the CO re-

sulting from a modified coupling to the counterion, and once it is sufficiently suppressed the ground state is singlet (Spin-Peierls) rather than antiferromagnetic. The observation that for $(TMTTF)_2SbF_6$ $dT_N/dP < 0$, is presumably associated with a competition with this non-magnetic ground state found at higher pressure. Further pressurization leads to the familiar sequence: another AF state and superconductivity. It is reasonable to ask whether this second, higher-pressure, AF state is a re-entrance of the phase described in Fig. 1, or whether it is a distinctly different symmetry breaking. The salts $(TMTTF)_2Br$ and $(TMTSF)_2PF_6$ should provide the answer, as they are understood to be representative of that portion of the phase diagram where the second

AF phase appears. X-ray scattering results²⁴ from the two materials provide evidence for a coexistence of weak charge and bond modulations, suggesting an even richer evolution of the phases than is presented in Fig. 5.

Acknowledgments

The research was supported by the National Science Foundation under grant number DMR-0203806. The authors are grateful for conversations with S. Brazovskii, S. Mazumda, P. Monceau, and H. Seo.

-
- * weiqiang@physics.ucla.edu
- ¹ D. Jerome and H. J. Schultz, *Advances in Physics* **51**, 293 (2002).
 - ² D. S. Chow, F. Zamborszky, B. Alavi, D. J. Tantillo, A. Baur, C. A. Merlic, and S. E. Brown, *Phys. Rev. Lett.* **85**, 1698 (2000).
 - ³ P. Monceau, F. Y. Nad, and S. Brazovskii, *Phys. Rev. Lett.* **86**, 4080 (2001).
 - ⁴ H. Seo and H. Fukuyama, *J. Phys. Soc. Japan* **66**, 1249 (1997).
 - ⁵ S. Mazumdar, S. Ramasesha, R. T. Clay, and D. K. Campbell, *Phys. Rev. Lett.* **82**, 1522 (1999).
 - ⁶ J. Riera and D. Poilblanc, *Phys. Rev. B* **63**, 241102 (2001).
 - ⁷ R. T. Clay, S. Mazumdar, and D. K. Campbell, *Phys. Rev. B* **67**, 115121 (2003).
 - ⁸ S. Brazovskii, P. Monceau, and F. Nad, *Synth. Metals* **137**, 1331 (2003).
 - ⁹ S. Mazumdar, R. T. Clay, and D. K. Campbell, *Phys. Rev. B* **62**, 13400 (2000).
 - ¹⁰ F. Y. Nad and P. Monceau, *J. Phys. IV* **12**, 133 (2002).
 - ¹¹ T. Nakamura, *J. Phys. Soc. Japan* **72**, 213 (2003).
 - ¹² F. Zamborszky, W. Yu, W. Raas, S. E. Brown, B. Alavi, C. A. Merlic, and A. Baur, *Phys. Rev. B* **66**, 081103 (2002).
 - ¹³ W. Yu, F. Zamborszky, B. Alavi, A. Baur, C. A. Merlic, and S. E. Brown, cond-mat/0312387.
 - ¹⁴ C. A. Merlic, A. Baur, D. J. Tantillo, and S. E. Brown, *Synth. Commun.* **29**, 2953 (1999).
 - ¹⁵ R. R. Ernst, G. Bodenhausen, and A. Wokaun, *Principles of nuclear magnetic resonance in one and two dimensions* (Oxford University Press, Oxford, 1990), pp. 360–366.
 - ¹⁶ Two inequivalent, coupled $I = 1/2$ spins produce a spectrum with four lines. The Hamiltonian is given by $H = \omega_1 I_{1z} + \omega_2 I_{2z} + \omega_{12} I_{1z} I_{2z}$, and the lines appear at frequencies $\sqrt{\omega_1^2 + \omega_{12}^2} \pm \omega_{12}/2$, $\sqrt{\omega_2^2 + \omega_{12}^2} \pm \omega_{12}/2$.
 - ¹⁷ V. J. McBrierty, D. C. Douglass, F. Wudl, and E. Aharon-Shalom, *Phys. Rev. B* **26**, 4805 (1982).
 - ¹⁸ J. P. Pouget and S. Ravy, *J. Phys. I* **6**, 1501 (1996).
 - ¹⁹ C. P. Slichter, *Principles of nuclear magnetic resonance* (Springer-Verlag, Berlin, 1996), pp. 592–595, 3rd ed.
 - ²⁰ P. Monceau, (private communication).
 - ²¹ W. Yu, F. Zhang, F. Zamborszky, B. Alavi, A. Baur, C. A. Merlic, and S. E. Brown, (unpublished).
 - ²² J. Riera and D. Poilblanc, *Phys. Rev. B* **62**, 16243 (2000).
 - ²³ M. Kuwabara, H. Seo, and M. Ogata, *J. Phys. Soc. Japan* **72**, 225 (2003).
 - ²⁴ J. P. Pouget and S. Ravy, *Synth. Metals* **85**, 1523 (1997).